# Equation of State and Phase Transition of the Spherical Lattice Gas*

WALTER PRESSMAN
*U. S. Army Signal Research and Development Laboratory, Fort Monmouth, New Jersey*

AND

JOSEPH B. KELLER
*Institute of Mathematical Sciences, New York University, New York, New York*

(Received April 6, 1960)

The spherical lattice gas is a modification of the ordinary lattice gas in which the occupation number of each cell is permitted to be any real number rather than $\pm 1$. However, the sum of squares of the occupation numbers is required to equal the number of cells. This permits one to evaluate the partition function by integrating over the surface of a certain sphere rather than by summing over lattice points on that surface. The partition function and the equation of state of the gas are evaluated in this way. It is found that in three dimensions the gas condenses, but not in one or two dimensions. Graphs of the phase transition curve and of the isotherms in three, two, and one dimension are presented.

The analytical work is simplified by taking advantage of the relationship between the properties of the lattice gas and of the Ising model of a ferromagnet. This relationship, demonstrated by C. N. Yang and T. D. Lee for the ordinary lattice gas and Ising model, also applies to the spherical lattice gas and the spherical model of a ferromagnet. The properties of the latter have been evaluated by T. H. Berlin and M. Kac. Graphs of the isotherms of the spherical model of the magnet, which were found in the course of the work, are also presented.

## 1. INTRODUCTION

THE spherical lattice gas is a simplified model of a gas. We introduce it because we can deduce its equation of state statistical-mechanically. We find that it undergoes phase transition in three dimensions, although not in one or two dimensions. We also find that its isotherms and transition curve, shown in Fig. 9, are in qualitative agreement with experimental curves. However, they exhibit a physically unreasonable negative pressure at very large and very small specific volumes. This can be traced to an inadequacy of the model for such specific volumes.

The ordinary lattice gas is defined by first dividing the volume $V$, which the gas occupies, into $V$ identical cells (e.g., cubes), each of unit volume. The potential energy of interaction between two molecules of the gas is defined to be infinite if they occupy the same cell, to be $-4J<0$ if they occupy cells which are nearest neighbors, and to be zero otherwise. Thus at most one particle can occupy each cell. Therefore the distribution of particles can be described by the $V$ coordinates $\sigma_1, \sigma_2, \cdots, \sigma_V$ where $\sigma_i=+1$ if cell $i$ is occupied and $\sigma_i=-1$ if it is not. By analogy, we define the spherical lattice gas by permitting each $\sigma_i$ to have any real value, but requiring that the $\sigma_i$ lie on the sphere

$$\sum_{i=1}^{V} \sigma_i^2 = V. \tag{1}$$

Then the grand partition function $Q_{SG}$ of the spherical lattice gas is obtained from that for the ordinary lattice gas by replacing sums over lattice points which lie on the sphere (1) by integrals over that sphere.

We were led to introduce the spherical lattice gas by the work of Yang and Lee[1] and that of Berlin and Kac.[2] Yang and Lee showed that $Q_G$, the grand partition function of the ordinary lattice gas, could be expressed in terms of $Q_I$, the partition function of the Ising model of ferromagnetism in a magnetic field $H$. But $Q_I$ has not been evaluated for a three-dimensional magnet nor for a two-dimensional one with $H\neq 0$, although the spontaneous magnetization is known as a function of temperature in the two-dimensional case. Therefore the phase transition curve of the two-dimensional lattice gas could be determined, but not the isotherms, while nothing could be found for the three-dimensional case.

Berlin and Kac introduced the spherical Ising model, which is related to the ordinary Ising model as the spherical lattice gas is to the ordinary lattice gas. They were able to evaluate its partition function $Q_{SI}$ for any value of $H$ in one, two and three dimensions. It exhibits spontaneous magnetization in three dimensions but not in one or two dimensions.

We noticed that the method of Berlin and Kac could be used to evaluate the grand partition function of the spherical lattice gas. We also noticed that $Q_{SG}$ is related to $Q_{SI}$ in the same way that $Q_G$ is related to $Q_I$. Therefore we could actually use their results to obtain the value of $Q_{SG}$.

In the course of our analysis of the isotherms and transition curve of the spherical lattice gas, we were led to examine the magnetization curves and spon-

* This article is based upon Research Report No. HT-5, Institute of Mathematical Sciences, New York University, 1960 (unpublished). This work was supported in part by the Air Force Office of Scientific Research of the Air Research and Development Command and as part of a cooperative activity between the U. S. Army Signal Research and Development Laboratory and the Institute of Mathematical Sciences.

[1] C. N. Yang and T. D. Lee, Phys. Rev. **87**, 410 (1952).
[2] T. H. Berlin and M. Kac, Phys. Rev. **86**, 821 (1952).

taneous magnetization of the spherical Ising model. Therefore these curves are also included.

Berlin, Witten, and Gersch[3] have studied a cellular model of the imperfect gas. In it the numbers of particles in the cells are taken as the statistical variables. Their partition function, like ours, involves an integral of the exponential of a quadratic form. However, whereas our integration extends over a hypersphere, theirs extends over a hyperplane. Their integrand includes a weighting factor which damps their integrand when it deviates from the average configuration of one particle per cell. In three dimensions their model exhibits condensation-like behavior below a critical temperature. There the $p$-$v$ isotherms are nonanalytic functions of $v$ consisting of three pieces. However, the condensation region is not characterized by constant pressure, and for temperatures sufficiently low the isotherms show thermodynamic instability. Thus their condensation phenomena are rather different from ours.

## 2. BASIC FORMULAS

The grand partition function of the lattice gas is[4]

$$Q_G(V,\mathcal{J},y)=\sum_{\sigma_1=\pm1}\cdots\sum_{\sigma_V=\pm1}\exp\left[\frac{\mathcal{J}}{2}\sum_{i,j=1}^{V}a_{ij}\sigma_i\sigma_j\right]\times\exp\left[(c\mathcal{J}+\tfrac{1}{2}\ln y)\sum_{j=1}^{V}\sigma_j\right]\exp\left[\tfrac{1}{2}(c\mathcal{J}+\ln y)V\right]. \quad (2)$$

Here $\sigma_i$ equals $+1$ if cell $i$ is occupied by a particle and $-1$ if it is not. We note that the $\sigma_i$ satisfy (1) and

$$\sigma_i^2=1. \quad (3)$$

The constant $\mathcal{J}$ is defined in terms of Boltzmann's constant $k$ and the absolute temperature $T$ by

$$\mathcal{J}=J/kT. \quad (4)$$

The quantity $a_{ij}$ equals $+1$ if cells $i$ and $j$ are nearest neighbors and is zero otherwise, while $c$ is the number of nearest neighbors of a cell. For cubic cells in one, two, and three dimensions $c$ equals two, four, and six, respectively. The fugacity is denoted by $y$.

From the definition of the spherical lattice gas, its grand partition function is

$$Q_{SG}(V,\mathcal{J},y)=\int_\Sigma\cdots\int d\sigma_1\cdots d\sigma_V\exp\left[\frac{\mathcal{J}}{2}\sum_{i,j=1}^{V}a_{ij}\sigma_i\sigma_j\right]\times\exp\left[(c\mathcal{J}+\tfrac{1}{2}\ln y)\sum_{j=1}^{V}\sigma_j\right]\exp\left[\tfrac{1}{2}(c\mathcal{J}+\ln y)V\right], \quad (5)$$

where $\Sigma$ represents the spherical surface $\sum\sigma_i^2=V$.

[3] T. H. Berlin, L. Witten, and H. A. Gersch, Phys. Rev. **92**, 189 (1953).

[4] G. F. Newell and E. W. Montroll, Revs. Modern Phys. **25**, 353 (1953).

The partition function for the Ising model of ferromagnetism is[5]

$$Q_I(N,\mathcal{J},\mathcal{H})=\sum_{\sigma_1=\pm1}\cdots\sum_{\sigma_N=\pm1}\times\exp\left[\frac{\mathcal{J}}{2}\sum_{i,j=1}^{N}a_{ij}\sigma_i\sigma_j+\mathcal{H}\sum_{j=1}^{N}\sigma_j.\right] \quad (6)$$

In (6) $N$ is the total number of lattice sites and

$$\mathcal{H}=\mu_0H/kT. \quad (7)$$

Here $\mu_0$ is the magnetic moment per particle. The partition function for the spherical model of ferromagnetism is[6]

$$Q_{SI}(N,\mathcal{J},\mathcal{H})=\int_\Sigma\cdots\int d\sigma_1\cdots d\sigma_N\times\exp\left[\frac{\mathcal{J}}{2}\sum_{i,j=1}^{N}a_{ij}\sigma_i\sigma_j+\mathcal{H}\sum_{j=1}^{N}\sigma_j\right]. \quad (8)$$

In (2) let us replace $V$ by $N$ and set

$$\ln y=2[\mathcal{H}-c\mathcal{J}].$$

Then by comparing (2) with (6) we obtain the following relationship, first obtained by Yang:

$$Q_G(N,\mathcal{J},\exp[2(\mathcal{H}-c\mathcal{J})])=\exp[\mathcal{H}-\tfrac{1}{2}c\mathcal{J}]Q_I(N,\mathcal{J},\mathcal{H}). \quad (9)$$

Upon comparing (5) and (8) we obtain the corresponding relation for the spherical models,

$$Q_{SG}(N,\mathcal{J},\exp[2(\mathcal{H}-c\mathcal{J})])=\exp[\mathcal{H}-\tfrac{1}{2}c\mathcal{J}]Q_{SI}(N,\mathcal{J},\mathcal{H}). \quad (10)$$

From either (9) or (10) it follows that[7] the thermodynamic properties of the lattice gas are related to those of the magnet. These relations are the same for the spherical and the original models. They are

$$p^*(\mathcal{J},\mathcal{H})=(F+\mathcal{H})/\mathcal{J}-\tfrac{1}{2}c, \quad (11)$$

$$v(\mathcal{J},\mathcal{H})=2/(1+\mathfrak{M}). \quad (12)$$

Here $p^*=p/J$ where $p$ is the pressure of the gas, $v$ is its specific volume, and $\mathfrak{M}=M/\mu_0$ where $M$ is the magnetization of the magnet. $F$, the limiting free energy per particle of the magnet, is defined by

$$F(\mathcal{H},\mathcal{J})=\lim_{N\to\infty}\frac{1}{N}\ln Q. \quad (13)$$

Here $Q$ denotes either $Q_I$ or $Q_{SI}$. $\mathfrak{M}$ is given by

$$\mathfrak{M}(\mathcal{H},\mathcal{J})=\frac{\partial F}{\partial\mathcal{H}}. \quad (14)$$

[5] See reference 4, p. 353.

[6] See reference 2, p. 827.

[7] See reference 4, p. 384.

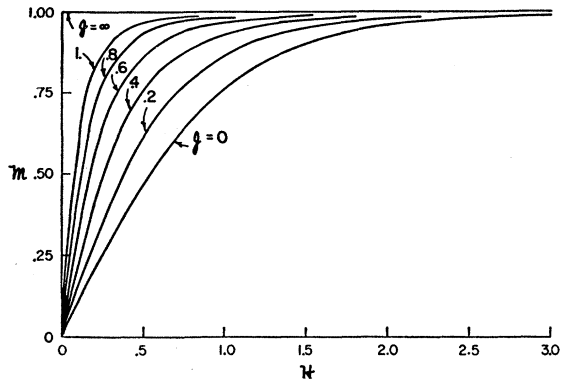


FIG. 1. Isotherms of the one-dimensional Ising model of a ferromagnet. The curves, based on Eq. (20), give the normalized magnetization $\mathfrak{M}=M/\mu_0$ as a function of the normalized external field $\mathcal{H}=H/kT$ for constant values of $\mathcal{J}=J/kT$. Since $\mathfrak{M}$ is an odd function of $\mathcal{H}$, only the non-negative values of $\mathcal{H}$ are shown.

Equations (11) and (12) are the parametric form of the equation of state of either the lattice gas or the spherical lattice gas. The parameter is $\mathcal{H}$, which ranges from minus infinity to plus infinity.

To obtain the equation of state of the spherical lattice gas we must insert $F(\mathcal{H},\mathcal{J})$, the limiting free energy per particle of the spherical Ising model, into (11) and (14) and then use (14) in (12). For a simple cubic lattice in $n$ dimensions ($n=1,2,3$), Berlin and Kac[2] have evaluated this free energy which we denote by $F_n(\mathcal{H},\mathcal{J})$. They obtain

$$F_n(\mathcal{H},\mathcal{J})=\tfrac{1}{2}\ln\left(\frac{\pi}{\mathcal{J}}\right)-\tfrac{1}{2}f_n(z)+\mathcal{J}z+\frac{\mathcal{H}^2}{4\mathcal{J}(z-n)}. \quad (15)$$

In (15) we have omitted an additive constant which occurs in reference 2 due to multiplication of $Q_{SI}$ by a normalization factor. Here $z$ is a real positive solution of the equation

$$2\mathcal{J}=\frac{\mathcal{H}^2}{2\mathcal{J}(z-n)^2}+\frac{df_n(z)}{dz}. \quad (16)$$

The function $f_n(z)$ is defined by

$$f_n(z)=\frac{1}{(2\pi)^n}\int_0^{2\pi}\cdots\int_0^{2\pi}dw_1\cdots dw_n \times\ln\left[z-\sum_{j=1}^{n}\cos w_j\right]. \quad (17)$$

It will prove convenient later to note that (16) implies $dF_n(z)/dz=0$ and that $z$ is an even function of $\mathcal{H}$. Then (15) shows that $F_n$ is also an even function of $\mathcal{H}$.

The equation of state of the spherical Ising model of a magnet is obtained by inserting (15) into (14). It is

$$\mathfrak{M}(\mathcal{H},\mathcal{J})=\mathcal{H}/2\mathcal{J}(z-n). \quad (18)$$

From (18) we see that $\mathfrak{M}$ is an odd function of $\mathcal{H}$. In the following sections we shall examine the equation of state of the spherical lattice gas and of the spherical Ising model in detail on the basis of the above equations.

In order to compare the properties of the spherical lattice gas with those of the lattice gas, we must determine the properties of the latter. We can do this in the one-dimensional case. The limiting free energy per

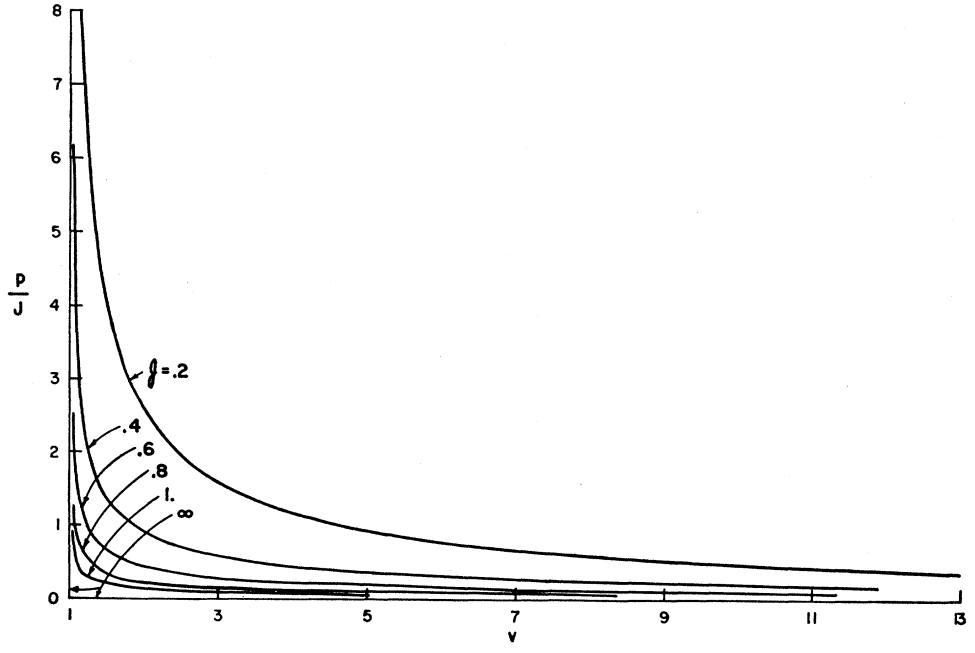


FIG. 2. Isotherms of the one-dimensional lattice gas based on Eqs. (22) and (23). The curves show the normalized pressure $p^*=p/J$ as a function of specific volume $v$ for various values of $\mathcal{J}=J/kT$.

particle of the one-dimensional Ising model $F_{1I}$, is[8]

$$F_{1I}(\mathcal{K},\mathcal{J})=\ln\{\exp\mathcal{J}\cosh\mathcal{K}+[\exp(2\mathcal{J})\sinh^2\mathcal{K}+\exp(-2\mathcal{J})]^{\frac{1}{2}}\}. \quad (19)$$

Upon substituting (19) into (14) we obtain

$$\mathfrak{M}_{1I}(\mathcal{K},\mathcal{J})=[\sinh^2\mathcal{K}+\exp(-4\mathcal{J})]^{-\frac{1}{2}}\sinh\mathcal{K}. \quad (20)$$

(This formula is misprinted in reference 4.) From (20) we deduce, omitting the subscripts,

$$\mathfrak{M}(\mathcal{K},0)=\tanh\mathcal{K}; \quad (21a)$$

$$\mathfrak{M}(\mathcal{K},\infty)=1, \quad \mathcal{K}>0; \quad (21b)$$

$$\mathfrak{M}(0,\mathcal{J})=0, \quad \mathcal{J}<\infty; \quad (21c)$$

$$\mathfrak{M}(\infty,\mathcal{J})=1. \quad (21d)$$

Equation (21c) demonstrates the well-known fact that spontaneous magnetization does not occur in the one-dimensional Ising model. Magnetization curves based on (20) are shown in Fig. 1. Less complete graphs are given in reference 4.

Upon substituting (19) into (11) and (20) into (12) we obtain the equation of state of the one-dimensional lattice gas in parametric form,

$$p^*=\frac{1}{\mathcal{J}}\ln\{\exp\mathcal{J}\cosh\mathcal{K}+[\exp(2\mathcal{J})\sinh^2\mathcal{K}+\exp(-2\mathcal{J})]^{\frac{1}{2}}+\mathcal{K}\}-1, \quad (22)$$

$$v=2\{1+[\sinh^2\mathcal{K}+\exp(-4\mathcal{J})]^{-\frac{1}{2}}\sinh\mathcal{K}\}^{-1}. \quad (23)$$

Isotherms of the one-dimensional lattice gas based on (22) and (23) are shown in Fig. 2. We see from (23) that as $\mathcal{K}$ varies from $+\infty$ to $-\infty$, $v$ varies continuously and hence no phase transition occurs. We also obtain easily the values listed in Table I. We see that the equations of state of the one-dimensional Ising model and of the one-dimensional lattice gas are physically quite reasonable.

### 3. THE ONE-DIMENSIONAL SPHERICAL LATTICE GAS

Since the properties of the spherical lattice gas can be found in terms of those of the spherical Ising model, we shall first examine that model. Its equation of state is given by (16) and (18) which become, in one dimension,

$$2\mathcal{J}=\frac{\mathcal{K}^2}{2\mathcal{J}(z-1)^2}+\frac{1}{(z^2-1)^{\frac{1}{2}}}, \quad (24)$$

$$\mathfrak{M}=\mathcal{K}/2\mathcal{J}(z-1). \quad (25)$$

From (24) and (25) we find that

$$\mathfrak{M}(\mathcal{K},0)=2\mathcal{K}[1+(1+4\mathcal{K}^2)^{\frac{1}{2}}]^{-1}; \quad (26a)$$

$$\mathfrak{M}(\mathcal{K},\infty)=1, \quad \mathcal{K}>0; \quad (26b)$$

$$\mathfrak{M}(0,\mathcal{J})=0, \quad \mathcal{J}<\infty; \quad (26c)$$

$$\mathfrak{M}(\infty,\mathcal{J})=1. \quad (26d)$$

The proofs of these results are similar to, but simpler than, those given in Appendix B for the three-dimensional case. Equation (26c) shows that spontaneous magnetization does not occur in this case. Magnetization curves of the spherical Ising model, based on (24) and (25), are shown in Fig. 3. For a given $\mathcal{K}$ and $\mathcal{J}$, the magnetization of the spherical model is less than that of the Ising model (Fig. 1).

From (11) and (15) we obtain for the spherical lattice gas in one dimension

$$p^*(\mathcal{J},\mathcal{K})=(F_1+\mathcal{K})/\mathcal{J}-1, \quad (28)$$

$$F_1(\mathcal{K},\mathcal{J})=\tfrac{1}{2}\ln\left(\frac{\pi}{\mathcal{J}}\right)-\tfrac{1}{2}\ln\tfrac{1}{2}[z+(z^2-1)^{\frac{1}{2}}]+\mathcal{J}z+\frac{\mathcal{K}^2}{4\mathcal{J}(z-1)}. \quad (29)$$

From (12) and (25) we obtain

$$v(\mathcal{J},\mathcal{K})=2\{1+\mathcal{K}/[2\mathcal{J}(z-1)]\}^{-1}. \quad (30)$$

Equations (28)–(30) express the equation of state of the one-dimensional spherical lattice gas in terms of the parameter $\mathcal{K}$. The quantity $z$ is defined as a root of (24).

TABLE I. Three pairs of values of $\mathcal{K}$ and $\mathfrak{M}$ for the one-dimensional Ising model of a ferromagnet and the corresponding pairs of values of $v$ and $p^*$ for the one-dimensional lattice gas.

| $\mathcal{K}$ | $\mathfrak{M}$ | $v$ | $p^*$ |
|---|---|---|---|
| $+\infty$ | $+1$ | 1 | $\sim 2\mathcal{K}/\mathcal{J}\to+\infty$ |
| 0 | 0 | 2 | $(1/\mathcal{J})\ln(2\cosh\mathcal{J})-1$ |
| $-\infty$ | $-1$ | $+\infty$ | 0 |

[8] See reference 4, p. 385.

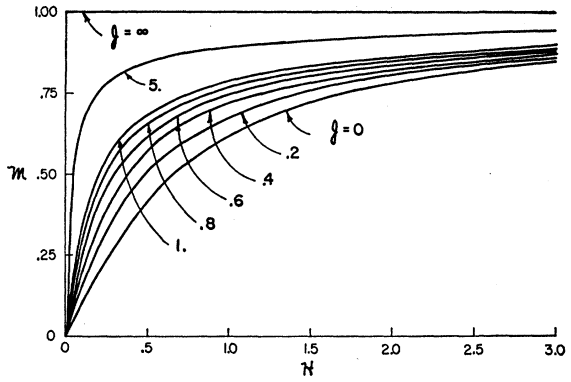


FIG. 3. Isotherms of the one-dimensional spherical model of a ferromagnet based on Eqs. (24) and (25). The normalized magnetization $\mathfrak{M}=M/\mu_0$ is shown as a function of the normalized external field $\mathcal{K}=H/kT$ for various constant values of $\mathcal{J}=J/kT$. These curves lie below the corresponding ones of the Ising model shown in Fig. 1.

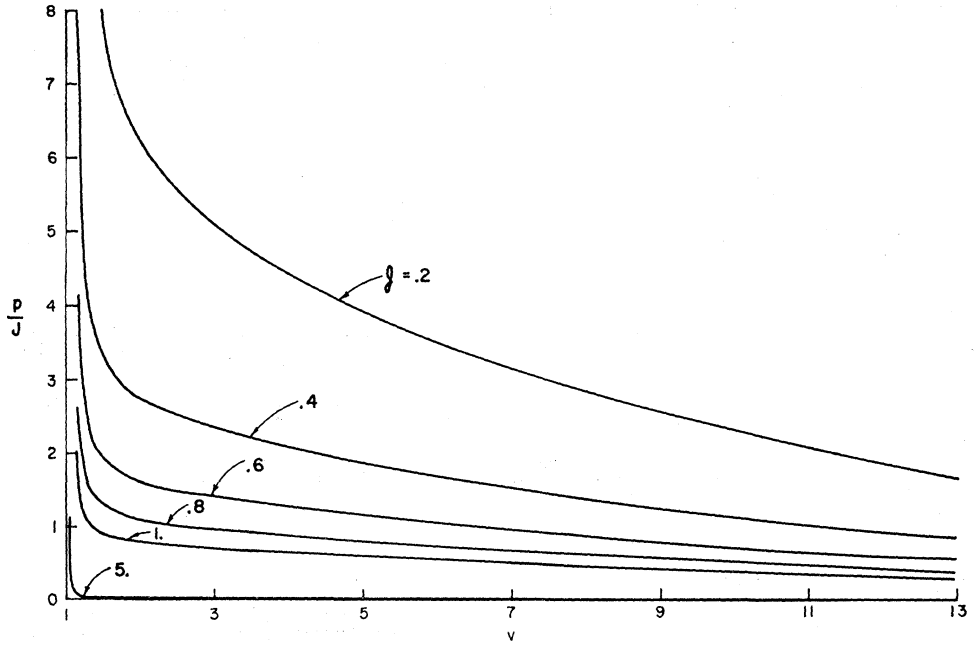


FIG. 4. Isotherms of the one-dimensional spherical lattice gas based on Eqs. (28)–(30). The curves show the normalized pressure $p^*=p/J$ as a function of specific volume $v$ for various values of $\mathcal{g}=J/kT$. Each isotherm crosses the axis $p^*=0$ for a sufficiently large value of $v$ indicating the inadequacy of the model for such large values of $v$.

Isotherms of the one-dimensional spherical lattice gas based on (28)–(30) are shown in Fig. 4. The method of computation used in preparing this and the subsequent figures is explained in Appendix A. Since spontaneous magnetization does not occur in the spherical magnet, phase transition does not occur in the spherical lattice gas. Much as in Appendix B we obtain the special results shown in Table II. We note from the third line of the table that when $v$ becomes large, $p$ becomes negative. Furthermore for large $v$ the isotherms corresponding to large values of $\mathcal{g}$ lie below those corresponding to smaller values of $\mathcal{g}$. This unphysical behavior of the equation of state for large $v$ is due to the inadequacy of the spherical model in this limit.

## 4. THE TWO-DIMENSIONAL SPHERICAL LATTICE GAS

For $n=2$, Eqs. (16) and (18) for the spherical Ising model become

$$2\mathcal{g}=\mathcal{H}^2/2\mathcal{g}(z-2)^2+(2/\pi z)K(2/z), \tag{31}$$

$$\mathfrak{M}(\mathcal{H},\mathcal{g})=\mathcal{H}/2\mathcal{g}(z-2). \tag{32}$$

In (31), $K(a)$ is the complete elliptic integral of the first kind, $0\leq a\leq 1$. From (31) and (32) we find that (26) is still valid for $n=2$. This is shown as in Appendix B by using the facts that $K(0)=\pi/2$ and $K(1)=\infty$. From (26c) we see that spontaneous magnetization does not occur for the spherical Ising model when $n=2$. The Ising model, however, does exhibit spontaneous magnetization when $n=2$. Magnetization curves based on (31) and (32) are shown in Fig. 5.

To obtain the equation of state of the spherical lattice gas in two dimensions, we set $n=2$ in (11) and (15) which become

$$p^*(\mathcal{g},\mathcal{H})=(F_2+\mathcal{H})/\mathcal{g}-2, \tag{34}$$

$$F_2(\mathcal{H},\mathcal{g})=\tfrac{1}{2}\ln\frac{\pi}{\mathcal{g}}-\tfrac{1}{2}f_2(z)+\mathcal{g}z+\frac{\mathcal{H}^2}{4\mathcal{g}(z-2)}. \tag{35}$$

Here $f_2(z)$ is defined by

$$f_2(z)=\frac{1}{(2\pi)^2}\int_0^{2\pi}\int_0^{2\pi}dw_1dw_2\ln[z-\cos w_1-\cos w_2].$$

Upon integrating once, $f_2(z)$ becomes

$$f_2(z)=\frac{1}{\pi}\int_0^{\pi}dw\ln\tfrac{1}{2}\{(z-\cos w)+[(z-\cos w)^2-1]^{\frac{1}{2}}\}. \tag{36}$$

TABLE II. Three pairs of values of $\mathcal{H}$ and $\mathfrak{M}$ for the one-dimensional spherical model of a ferromagnet and the corresponding pairs of values of $v$ and $p^*$ for the one-dimensional spherical lattice gas.

| $\mathcal{H}$ | $\mathfrak{M}$ | $v$ | $p^*$ |
|---|---|---|---|
| $+\infty$ | 1 | 1 | $\sim\frac{2\mathcal{H}}{\mathcal{g}}\to+\infty$ |
| 0 | 0 | 2 | $\frac{1}{2\mathcal{g}}\left\{(1+4\mathcal{g}^2)^{\frac{1}{2}}-\ln\frac{1}{4\pi}[(1+4\mathcal{g}^2)^{\frac{1}{2}}]\right\}-1$ |
| $-\infty$ | $-1$ | $+\infty$ | $\sim-\frac{\ln\lvert\mathcal{H}\rvert}{2\mathcal{g}}\to-\infty$ |

From (12) and (32) we obtain

$$v(\mathcal{J},\mathcal{H})=2[1+\mathcal{H}/2\mathcal{J}(z-2)]^{-1}. \tag{37}$$

Isotherms of the two-dimensional spherical lattice gas based on (34)–(37) are shown in Fig. 6. From (26), (34), and (37), by considerations like those in Appendix B, we obtain the special results in Table III. Here $z_m$ is the solution of Eq. (3) in Appendix C. We see from the third line of the table that for large $v$ the behavior of the two-dimensional spherical lattice gas is unphysical, just as in the one-dimensional case.

## 5. THE THREE-DIMENSIONAL SPHERICAL LATTICE GAS

In three dimensions, (16) and (18) for the spherical Ising model become

$$2\mathcal{J}=\frac{\mathcal{H}^2}{2\mathcal{J}(z-3)^2}+\frac{df_3(z)}{dz}, \tag{38}$$

$$\mathfrak{M}(\mathcal{H},\mathcal{J})=\mathcal{H}/2\mathcal{J}(z-3). \tag{39}$$

In (38), $df_3/dz$ is given by

$$\frac{df_3(z)}{dz}=\frac{1}{(2\pi)^3}\int_0^{2\pi}\int_0^{2\pi}\int_0^{2\pi}\frac{dw_1dw_2dw_3}{z-\cos w_1-\cos w_2-\cos w_3}$$
$$=\frac{1}{\pi^2}\int_0^{\pi}dw\left(\frac{2}{z-\cos w}\right)K\left(\frac{2}{z-\cos w}\right). \tag{40}$$

In Appendix B we show that

$$\mathfrak{M}(\mathcal{H},0)=2\mathcal{H}[1+(1+4\mathcal{H}^2)^{\frac{1}{2}}]^{-1}; \tag{41a}$$

$$\mathfrak{M}(\mathcal{H},\infty)=1, \quad \mathcal{H}>0; \tag{41b}$$

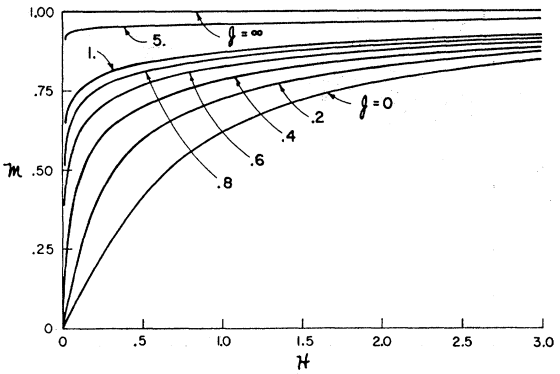


FIG. 5. Isotherms of the two-dimensional spherical model of a ferromagnet based on Eqs. (31) and (32). The normalized magnetization $\mathfrak{M}=M/\mu_0$ is shown as a function of the normalized external field $\mathcal{H}=H/kT$ for various constant values of $\mathcal{J}=J/kT$.

$$\mathfrak{M}(0+,\mathcal{J})=\left(1-\frac{\mathcal{J}_c}{\mathcal{J}}\right)^{\frac{1}{2}} \quad \text{for} \quad \mathcal{J}>\mathcal{J}_c=0.2527\cdots; \tag{41c}$$

$$\mathfrak{M}(0,\mathcal{J})=0 \quad \text{for} \quad \mathcal{J}<\mathcal{J}_c; \tag{41d}$$

$$\mathfrak{M}(\infty,\mathcal{J})=1. \tag{41e}$$

Equations (41c) and (41d) show that spontaneous magnetization occurs for $\mathcal{J}>\mathcal{J}_c$.

In Appendix D it is proved that

$$\left.\frac{d\mathfrak{M}}{d\mathcal{H}}\right|_{\mathcal{H}=0}=1, \quad \mathcal{J}=0; \tag{42}$$

$$\left.\frac{d\mathfrak{M}}{d\mathcal{H}}\right|_{\mathcal{H}=0}=\frac{1}{2\mathcal{J}(z_m-3)}, \quad 0<\mathcal{J}<\mathcal{J}_c; \tag{43}$$

$$\left.\frac{d\mathfrak{M}}{d\mathcal{H}}\right|_{\mathcal{H}=0}=\infty, \quad \mathcal{J}>\mathcal{J}_c. \tag{44}$$

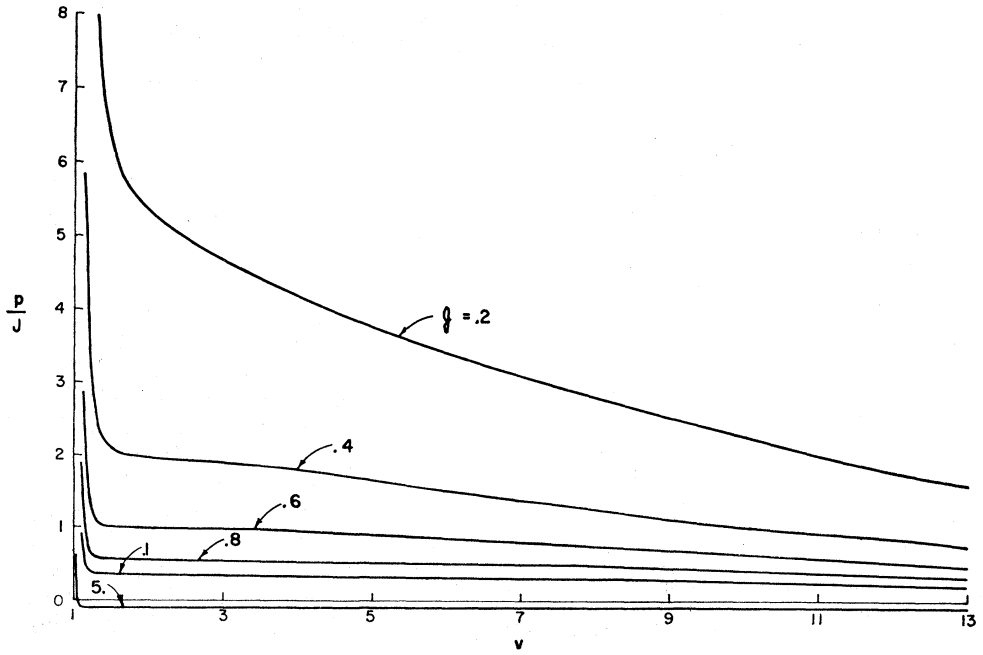


FIG. 6. Isotherms of the two-dimensional spherical lattice gas based on Eqs. (34)–(37). The curves show the normalized pressure $p^*=p/J$ as a function of specific volume $v$ for various values of $\mathcal{J}=J/kT$. Each isotherm crosses the axis $p^*=0$ for a sufficiently large value of $v$ indicating the inadequacy of the model for such large values of $v$.

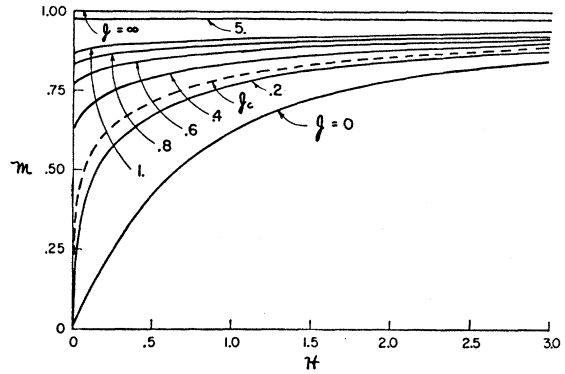


FIG. 7. Isotherms of the three-dimensional spherical model of a ferromagnet based on Eqs. (38)–(40). The normalized magnetization $\mathfrak{M}=M/\mu_0$ is shown as a function of the normalized external field $\mathcal{H}=H/kT$ for various constant values of $\mathcal{J}=J/kT$. Spontaneous magnetization occurs for $\mathcal{J}>\mathcal{J}_c=0.2527$. This is shown by the fact that for such values of $\mathcal{J}$, the magnetization is different from zero for $\mathcal{H}=0$.

Here $z_m$ is the solution of Eq. (4) of Appendix C. Magnetization curves based on (38)–(41) are shown in Fig. 7. The spontaneous magnetization curve based on (41c) is shown in Fig. 8.

The equation of state of the three-dimensional spherical lattice gas is now obtained by setting $n=3$ in (11) and (15) which become

$$p^*(\mathcal{J},\mathcal{H})=(F_3+\mathcal{H})/\mathcal{J}-3, \tag{45}$$

$$F_3(\mathcal{H},\mathcal{J})=\tfrac{1}{2}\ln\frac{\pi}{\mathcal{J}}-\tfrac{1}{2}f_3(z)+\mathcal{J}z+\frac{\mathcal{H}^2}{4\mathcal{J}(z-3)}. \tag{46}$$

Here $f_3(z)$ is given by

$$f_3(z)=\frac{1}{(2\pi)^3}\int_0^{2\pi}\int_0^{2\pi}\int_0^{2\pi} dw_1dw_2dw_3 \times\ln(z-\cos w_1-\cos w_2-\cos w_3). \tag{47}$$

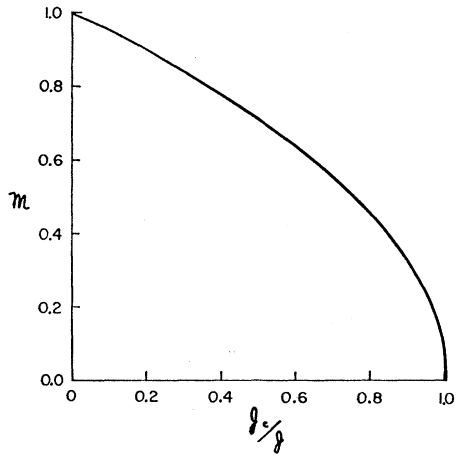


FIG. 8. Spontaneous magnetization of the three-dimensional spherical model of a ferromagnet based on Eq. (41c). The ordinate is the limiting value of the magnetization $\mathfrak{M}(\mathcal{H},\mathcal{J})$ as $\mathcal{H}$ tends to zero through positive values. It is just the intercept of the isotherms with the axis $\mathcal{H}=0$ in Fig. 7. The abscissa is $\mathcal{J}_c/\mathcal{J}$.

Equations (12) and (39) yield

$$v(\mathcal{J},\mathcal{H})=2[1+\mathcal{H}/2\mathcal{J}(z-3)]^{-1}. \tag{48}$$

From (41), (45), and (48) we derive, in Appendix C, the entries of Table IV. In this table $z_m$ is the solution of Eq. (4) of Appendix C, while $v_L$ and $v_G$ are determined by the equations

$$v_L=2[1+M(0+,\mathcal{J})]^{-1} \tag{49}$$

$$1/v_L+1/v_G=1. \tag{50}$$

For very small and very large $v$, the isotherms behave as they do in the one- and two-dimensional cases. However for $\mathcal{J}>\mathcal{J}_c$, a discontinuity occurs in the $p^*$, $v$ curves at the parameter value $\mathcal{H}=0$. At this value we obtain two different specific volumes for each $p^*$. We designate the smaller $v_L$ to indicate the value at which the liquid begins to vaporize. The larger we call $v_G$, which is the specific volume at which the gas begins to liquefy. The jump in specific volume is

$$v_G-v_L=4M(0+,\mathcal{J})/[1-M^2(0+,\mathcal{J})]. \tag{51}$$

TABLE III. Three pairs of values of $\mathcal{H}$ and $\mathfrak{M}$ for the two-dimensional spherical model of a ferromagnet and the corresponding pairs of values of $v$ and $p^*$ for two-dimensional spherical lattice gas.

| $\mathcal{H}$ | $\mathfrak{M}$ | $v$ | $p^*$ |
|---|---|---|---|
| $+\infty$ | 1 | 1 | $\frac{2\mathcal{H}}{\mathcal{J}}\to+\infty$ |
| 0 | 0 | 2 | $\frac{1}{2\mathcal{J}}\left\{\ln\frac{\pi}{\mathcal{J}}-f_2(z_m)+\mathcal{J}z_m\right\}-2$ |
| $-\infty$ | $-1$ | $+\infty$ | $-\frac{\ln\lvert\mathcal{H}\rvert}{2\mathcal{J}}\to-\infty$ |

We now eliminate $\mathcal{J}$ between (45) and (49), obtaining

$$p^*=\frac{2}{\mathcal{J}_c}\left(\frac{v_L-1}{v_L^2}\right)\left[\ln\left(\frac{v_L-1}{v_L^2}\right)+\ln\frac{4\pi}{\mathcal{J}_c}-f_3(3)\right], \quad 1\le v_L\le 2. \tag{52}$$

Equation (52) defines that half of the phase transition curve, or boundary of the two-phase region, in the $p^*$,$v$ plane at which the liquid begins to vaporize. The other half of this curve is obtained by eliminating $v_L$ from (52) by means of (50), which yields a relation between $p^*$ and $v_G$. This is the half of the phase transition curve at which the gas begins to liquify. The maximum of $p^*$ on this curve occurs at $v_L=v_G=2$, where $\partial p^*/\partial v_L=\partial p^*/\partial v_G=0$. It is interesting to note that at the maximum $\partial^2 p/\partial v_L^2=\partial^2 p/\partial v_G^2\neq 0$. Thus the phase transition curve is not as flat at its maximum as is that of the two-dimensional ordinary lattice gas. The phase

transition curve or two-phase boundary is shown as a dashed line in Fig. 9.

In order to examine the isotherms of the three-dimensional spherical lattice gas, we prove in Appendix D that

$$\left.\frac{dp^*}{dv}\right|_{v=2} = -(z_m-3), \quad \mathcal{J}<\mathcal{J}_c; \tag{53}$$

$$\left.\frac{dp^*}{dv}\right|_{v=v_L, v_G} = 0, \quad \mathcal{J}>\mathcal{J}_c. \tag{54}$$

From (54) we see that the isotherms meet the two-phase boundary with zero slope and that the compressibility is infinite at this boundary. The isotherms are shown in Fig. 9. The horizontal line within the two-phase region in that figure represents the discontinuity (51).

Although Fig. 9 bears a marked qualitative resemblance to the $p$, $v$ diagram of a real gas-liquid system, it is unrealistic for large $\mathcal{J}$ at small $v$ and for all $\mathcal{J}$ at large $v$. This is shown by the small negative trough of the condensation curve for $1\leq v\leq 2$ and by a corresponding one of the same depth but of infinite extent for large values of $v$.

### 6. FINAL REMARKS

Our method of computation of the isotherms from (45)–(48) is described in Appendix A. In this computation for each $\mathcal{J}$, values were assigned to the two parameters $z$ and $\mathfrak{IC}$, and corresponding values of $p^*$ and $v$ were computed. The values of $\mathfrak{IC}$ ranged from $-\infty$ to $+\infty$ and those of $z$ ranged from $z_m$ to $+\infty$. The minimum value $z_m$ is determined in Appendix C as a root of Eq. (1) of that Appendix. We now wish to determine whether the isotherms can be continued beyond the two-phase boundary by choosing $z<z_m$. If so, we wish to see if such a continuation has physical

TABLE IV. Five pairs of values of $\mathfrak{IC}$ and $\mathfrak{M}$ for the three-dimensional spherical model of a ferromagnet and the corresponding pairs of values of $v$ and $p^*$ for the three-dimensional spherical lattice gas. Since spontaneous magnetization occurs below the critical temperature ($\mathcal{J}>\mathcal{J}_c$), the value of $\mathfrak{IC}$ depends upon whether $\mathfrak{IC}$ tends to zero through positive or negative values. For the spherical lattice gas below the critical temperature on the condensation curve, the pressure is the same for $v=v_L$ as for $v=v_G$.

| $\mathfrak{IC}$ | | $\mathfrak{M}$ | $v$ | $p^*$ |
|---|---|---|---|---|
| $+\infty$ | | $+1$ | 1 | $\sim\frac{2\mathfrak{IC}}{\mathcal{J}}\to+\infty$ |
| $0\pm$ | ($\mathcal{J}<\mathcal{J}_c$) | 0 | 2 | $\frac{1}{2\mathcal{J}}\left[\ln\frac{\pi}{\mathcal{J}}+2\mathcal{J}z_m-f_3(z_m)\right]-3$ |
| $0+$ | ($\mathcal{J}>\mathcal{J}_c$) | $+\mathfrak{M}(0+,\mathcal{J})$ | $v_L$ | $\frac{1}{2\mathcal{J}}\left[\ln\frac{\pi}{\mathcal{J}}-f_3(3)\right]$ |
| $0-$ | ($\mathcal{J}>\mathcal{J}_c$) | $-\mathfrak{M}(0+,\mathcal{J})$ | $v_G$ | |
| $-\infty$ | | $-1$ | $+\infty$ | $\sim\frac{\ln\lvert\mathfrak{IC}\rvert}{2\mathcal{J}}\to-\infty$ |

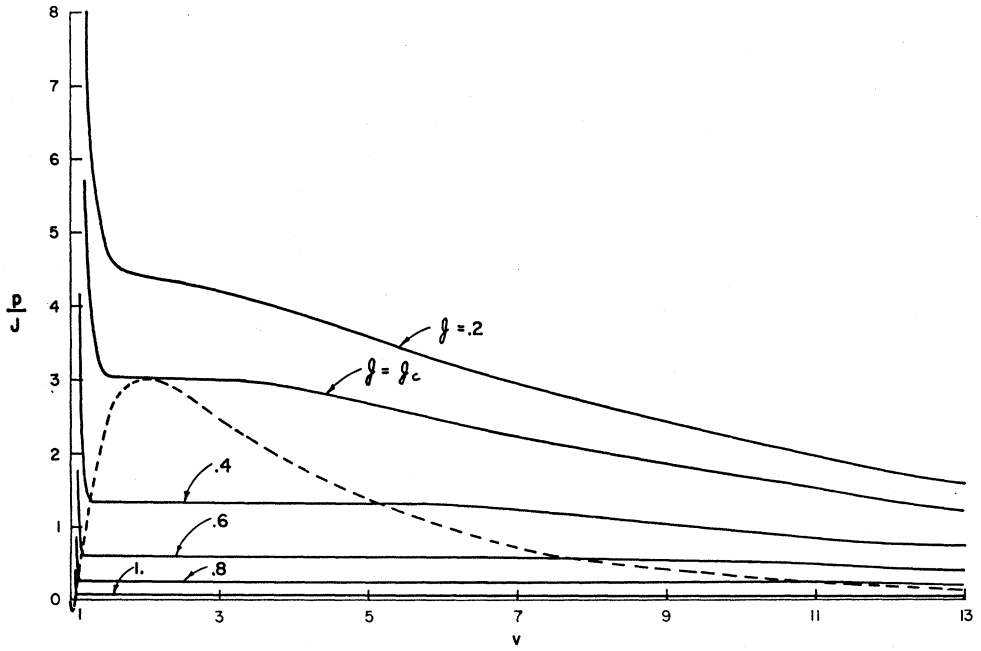


FIG. 9. Isotherms of the three-dimensional spherical lattice gas based on Eqs. (45)–(48). The curves show the normalized pressure $p^*=p/J$ as a function of specific volume $v$ for various values of $\mathcal{J}=J/kT$. Each isotherm crosses the axis $p^*=0$ for a sufficiently large value of $v$ indicating the inadequacy of the model for such large values of $v$. The dashed curve is the boundary of the two-phase region. Half of it is given by (52) and the other half by (50) and (52). The horizontal part of each isotherm in the two-phase region has been drawn to connect the end points of the two other portions of the isotherm. This horizontal part is not described by our equations, which do not yield any isotherms in this region.

significance. In particular, does it yield metastable states?

We first consider the spherical Ising model and write (16) and (18) in the form

$$\mathfrak{M}^2=1-\frac{1}{2\mathcal{J}}\frac{df_n}{dz}, \tag{55}$$

$$\mathcal{H}=2\mathcal{J}(z-n)\mathfrak{M}. \tag{56}$$

In one, two, and three dimensions the following remarks apply. If $n<z<z_m$, it follows that $(1/2\mathcal{J})df_n(z)/dz>1$. Then (55) shows that $\mathfrak{M}$ is imaginary. If $|z|<n$ then from (17) we find that $df_n/dz$ is infinite. Hence we need consider only $z\leq -n$.

From (17) we note that $df_n(z)/dz$ is an odd function of $z$. Therefore we replace $z$ by $-z$ in (55) and (56) and obtain

$$\mathfrak{M}^2=1+\frac{1}{2\mathcal{J}}\frac{df_n(z)}{dz}, \tag{57}$$

$$\mathcal{H}=-2\mathcal{J}\mathfrak{M}(z+n), \quad z>n. \tag{58}$$

Since $df_n/dz$ is finite and positive for $z>n$, (57) and (58) yield two real continuations for $\mathfrak{M}$ and $\mathcal{H}$ since two values of the square root can be used in (57). According to (58), $\mathfrak{M}$ and $\mathcal{H}$ have opposite signs for each solution, and from (57) $|\mathfrak{M}|>1$. Thus both of these continuations seem to be physically unrealistic.

We shall now consider the possibility of continuing the isotherms of the spherical lattice gas. First we consider the range $n<z<z_m$. Since $\mathfrak{M}$ is imaginary in this range, we see from (12) that $v$ will be complex. On the other hand, if $z<n$, (17) shows that $f_n(z)$ is complex. Then (15) and (11) show that $p^*$ is not real. Thus if $z$ and $\mathcal{H}$ are real, there is no real continuation of the isotherms.

Next we shall show that when $v$, $p^*$, and $\mathcal{J}$ are all real then $z$ and $\mathcal{H}$ must be real. To show this we first note that from (12), $\mathfrak{M}$ is real if $v$ is real. Then from (55) it follows that $z$ is real. For if $z$ were not real, by (17) $df_n/dz$ would not be real and then (55) would show that $\mathfrak{M}$ would not be real. Finally from (18), the reality of $z$ and $\mathfrak{M}$ imply that $\mathcal{H}$ is real. This result and that of the preceding paragraph show that, on the basis of our equations, there is no real continuation of the isotherms of the spherical lattice gas into the two-phase region. Thus the boundary of the two-phase region is the natural boundary of the function $p^*(v,\mathcal{J})$.

## APPENDIX A

### Method of Computation

Each isotherm of the spherical model of ferromagnetism and of the spherical lattice gas was computed by assigning a value to $\mathcal{J}$ and selecting a set of values for $z$. For these values $\mathfrak{M}$, $\mathcal{H}$, $v$, $F$, and $p^*$ were computed successively from (55), (56), (12), (15), and (11) using a Burroughs 220 electronic computer. The only difficulty was that of evaluating $f_n(z)$ and $df_n(z)/dz$ for $n=2$ and 3. The second term on the right side of (31), which gives $df_2/dz$, involves the complete elliptic integral of the first kind. This integral also occurs in (39) which gives $df_3/dz$. It was approximated by a formula of Hastings.[9] Then $df_3/dz$ was computed by numerical integration using Simpson's one-third rule, which was also used to compute $f_2(z)$ from (36).

The function $f_3(z)$ was computed from the series

$$f_3(z)=\ln z-\frac{3}{4z^2}-\frac{45}{32z^4}-\frac{155}{32z^6}-\frac{22\,365}{1024z^8}-\cdots. \tag{A.1}$$

This series can be derived by first writing (47) in the form

$$f_3(z)=\ln z-\sum_{n=1}^{\infty}\frac{A_n}{nz^n}. \tag{A.2}$$

The coefficients in (A.2) are found to be

$$A_n=\frac{1}{\pi^3}\int_0^{\pi}\int_0^{\pi}\int_0^{\pi}\left(\sum_{j=1}^{3}\cos\omega_j\right)^n d\omega_1 d\omega_2 d\omega_3. \tag{A.3}$$

The integral in (A.3) is expressible in terms of $I_0$, the modified Bessel function of the first kind of order zero. This yields

$$A_n=\lim_{a\to 0}\frac{d^n}{da^n}([I_0(a)]^3). \tag{A.4}$$

Since $I_0(a)$ is an even function of $a$, it follows from (A.4) that $A_n=0$ when $n$ is odd. Upon substitution of the power series for $I_0$ into (A.4) we obtain, for even $n=2s$,

$$\frac{A_{2s}}{2s}=\frac{(2s-1)!}{2^{2s}}\sum_{k=0}^{s}[(s-k)!]^{-2}\sum_{j=0}^{k}[j!(k-j)!]^{-2}. \tag{A.5}$$

If $A_{2s}$ is computed for $s=1, 2, 3, 4$ from (A.5) and the results are inserted into (A.2), the result is (A.1).

## APPENDIX B

### Limit Properties of the Three-Dimensional Spherical Magnet and the Spherical Lattice Gas

We shall now prove various statements made in the text about the behavior of the equations of state of the three-dimensional spherical models of the magnet and the lattice gas. Let us begin with (41). From (38) it follows that $z\to\infty$ when $\mathcal{J}\to 0$. Then from (38)–(40)

[9] C. Hastings, Jr., *Approximations for Digital Computers* (Princeton University Press, Princeton, New Jersey, 1955), p. 171.

we find that as $\mathcal{J} \to 0$,

$$2\mathcal{J} \sim \mathcal{H}^2/2\mathcal{J}z^2 + 1/z, \tag{B.1}$$

$$\mathfrak{M} \sim \mathcal{H}/2\mathcal{J}z. \tag{B.2}$$

We now solve (B.1) for $\mathcal{J}z$ and substitute the result into (B.2), which yields (41a).

To prove (41b) we first note from (38) that $z \to 3$ when $\mathcal{J} \to \infty$. We also note that $df_3(3)/dz = 2\mathcal{J}_c$, which was proved by Watson.[10] Then for $\mathcal{J}$ large, (38) can be written as

$$[\mathcal{H}/2\mathcal{J}(z-3)]^2 \sim 1 - \mathcal{J}_c/\mathcal{J}. \tag{B.3}$$

Thus

$$\lim_{\mathcal{J}\to\infty} \left[\frac{\mathcal{H}}{2\mathcal{J}(z-3)}\right] = 1,$$

which completes the proof. To prove (41d) we see from (17) that $df_3/dz$ decreases monotonically from $2\mathcal{J}_c$ at $z=3$ to zero at $z=\infty$ and that it behaves like $z^{-1}$ for large $z$. If $\mathcal{J} < \mathcal{J}_c$ and $\mathcal{H} \to 0$, it follows from (38) that $z \to z_m > 3$, where $z_m$ satisfies (C.4), and (41d) follows. If $\mathcal{J} > \mathcal{J}_c$ then $z \to 3$ in (38) when $\mathcal{H} \to 0$ and (38) becomes (B.3), proving (41c). To prove (41e) we observe from (38) that when $\mathcal{H} \to \infty$, $z \to \infty$ and consequently $df_3/dz \to 0$. Then

$$\lim_{\mathcal{H}\to\infty} \left[\frac{\mathcal{H}}{2\mathcal{J}(z-3)}\right] = 1. \tag{B.4}$$

This is (41e) and completes the proof of (41).

We shall now derive the values of $p^*$ in Table IV. When $\mathcal{H} \to \pm\infty$ it follows that $\mathfrak{M} \to \pm 1$, since $\mathfrak{M}$ is odd. Then from (B.4), $z \sim |\mathcal{H}|/2\mathcal{J} \to \infty$. For large $z$, $f_3(z) \sim \ln z = \ln(|\mathcal{H}|/2\mathcal{J})$. Substitution of these limiting values for $z$ and $f_3(z)$ into (46) as $|\mathcal{H}| \to \infty$ yields

$$F_3 \sim -\tfrac{1}{2}\ln(|\mathcal{H}|/2\mathcal{J}) + |\mathcal{H}|. \tag{B.5}$$

Substitution of (B.5) into (45) yields, when $\mathcal{H} \to +\infty$, the entry on line 1, column 4 of Table IV. When $\mathcal{H} \to -\infty$ this substitution yields the entry on line 4, column 4 of Table IV. When $\mathcal{H} \to \pm 0$ and $\mathcal{J} < \mathcal{J}_c$, $z \to z_m > 3$ and $H/2\mathcal{J}(z-3) \to 0$. Substitution of these values into (45) yields the entry on line 2, column 4 of Table IV. Finally when $\mathcal{H} \to \pm 0$ and $\mathcal{J} > \mathcal{J}_c$, $z \to z_m = 3$, $\mathcal{H}/2\mathcal{J}(z-3) \to \pm\mathfrak{M}(0+,\mathcal{J})$. Again, substituting these values into (45) yields line 3 of Table IV.

## APPENDIX C

### Determination of $z_m$

We know from (17) that $df_n(z)/dz$ is a positive monotonic decreasing function of $z$ behaving like $1/z$ for large $z$. We also know from (24) that $df_1(1)/dz = \infty$, from (31) that $df_2(2)/dz = \infty$, and from Appendix B that $df_3(3)/dz = 2\mathcal{J}_c$. Therefore $z_m$ corresponds to the smallest non-negative value of $\mathfrak{M}^2$ that can be realized from (55). For $n=1$, 2 and all $\mathcal{J}$ and for $n=3$, $\mathcal{J} < \mathcal{J}_c$ this is $\mathfrak{M}^2 = 0$. Hence under these conditions, $z_m$ is a solution of

$$\frac{df_n(z_m)}{dz} = 2\mathcal{J}. \tag{C.1}$$

More specifically

$$z_m = (1 + 1/4\mathcal{J}^2)^{\frac{1}{2}}, \quad n=1; \tag{C.2}$$

$$z_m = (1/\pi\mathcal{J})K(2/z_m), \quad n=2; \tag{C.3}$$

$$\frac{df_3(z_m)}{dz} = 2\mathcal{J}, \quad n=3,\ \mathcal{J} < \mathcal{J}_c. \tag{C.4}$$

From Appendix B we also have

$$z_m = 3, \quad n=3, \quad \mathcal{J} > \mathcal{J}_c. \tag{C.5}$$

In all cases $z_m \geq n$.

## APPENDIX D

### Shapes of the Isotherms of the Spherical Lattice Gas

The slope of the isotherms of the spherical lattice gas can be expressed simply in terms of the properties of the spherical model of a ferromagnet. To show this we differentiate (11) with respect to $v$ and (12) with respect to $\mathcal{H}$. Upon combining these two equations we obtain, after use of (14),

$$\frac{dp^*}{dv} = -\frac{(1+\mathfrak{M})^3}{2\mathcal{J}(d\mathfrak{M}/d\mathcal{H})}. \tag{D.1}$$

This relationship also relates the ordinary lattice gas and the Ising model.

Let us now evaluate $d\mathfrak{M}/d\mathcal{H}$ for the spherical model. To do so we differentiate (18) and (16) with respect to $\mathcal{H}$ and combine the two results. We then obtain for the spherical magnet

$$\frac{d\mathfrak{M}}{d\mathcal{H}} = \frac{1}{2\mathcal{J}(z-n)}\left\{-\frac{d^2f_n}{dz^2}\Big/\left(\frac{4\mathcal{J}\mathfrak{M}^2}{(z-n)} - \frac{d^2f_n}{dz^2}\right)\right\}. \tag{D.2}$$

Since $d^2f_n/dz^2 \leq 0$ it follows from (D.2) that $d\mathfrak{M}/d\mathcal{H} \geq 0$ and from (D.1) that $dp^*/dv \leq 0$.

Let us now deduce (42)–(44), (53), and (54). If $\mathcal{J}=0$, (42) follows directly from (41a). For $\mathcal{J}>0$ we have, for $z \sim 3$,[11]

$$\frac{d^2f_3(z)}{dz^2} \sim -[2^{\frac{3}{2}}\pi(z-3)^{\frac{1}{2}}]^{-1}. \tag{D.3}$$

From this equation and (17) it follows that $d^2f_3(z)/dz^2$ increases monotonically from $-\infty$ at $z=3$ to zero at $z=\infty$.

[10] G. N. Watson, Quart. J. Math. **10**, 266 (1939).

[11] See reference 2, p. 385.

If $0<\mathcal{J}<\mathcal{J}_c$ then, as is shown in Appendix C, when $\mathcal{K}\to 0$ it follows that $z\to z_m>3$ and $\mathfrak{M}\to 0$. Hence $d^2f_3(z)/dz^2\to d^2f_3(z_m)/dz^2\neq 0$. Upon substitution into (D.2) of the limits attained by $z$, $\mathfrak{M}$, and $d^2f_3(z)/dz^2$ as $\mathcal{K}\to 0$ we obtain (43). If $\mathcal{J}>\mathcal{J}_c$ then from Appendix C we find that as $\mathcal{K}\to 0$, $z\to 3$ and $\mathfrak{M}^2\to(1-\mathcal{J}_c/\mathcal{J})>0$. Hence from (D.3), $d^2f_3/dz^2\to-[2^{\frac{3}{2}}\pi(z-3)^{\frac{1}{2}}]^{-1}$. Substitution of these limiting values of $z$, $\mathfrak{M}$, and $d^2f_3(z)/dz^2$ into (D.2) yields (44).

Equation (53) then follows upon substitution of (41d) and (43) into (D.1), and (54) follows upon substitution of (41c) and (44) into (D.1).

PHYSICAL REVIEW VOLUME 120, NUMBER 1 OCTOBER 1, 1960

# Approximate Analytic Approach to the Classical Scattering Problem*

GUY W. LEHMAN AND KENNETH A. SHAPIRO†
*Atomics International, Canoga Park, California*
(Received May 25, 1960)

An approximate analytic approach to the problem of determining differential scattering cross sections for classical central-field repulsive forces is described. It is shown that the impact parameter, $b$, can be approximated by $b=R\cos(\theta/2)$, where $R$ is approximately the distance of closest approach and $\theta$ is the scattering angle in the center-of-mass system. A simple approximation gives the potential energy of interaction between two atoms as $V(R)=2E\sin(\theta/2)$, where $E$ is the energy in the center-of-mass system. Simple analytic expressions for the differential scattering cross section, $\sigma$, are derived from the above two relationships for three special cases of a two-parameter screened Coulomb potential energy,

$$V(R)=Z_1Z_2e^2A\exp(-pAR)[1-\exp(-AR)]^{-1},$$

where $Z_ie$ is the charge on the $i$th atom, $A^{-1}$ is a screening radius, and $p$ is an adjustable parameter which is restricted to $\frac{1}{2}$, 1, and 2 in this paper.

A new and improved method for calculating $\sigma$ exactly is also discussed and is used to compute the exact behavior of $\sigma$ for $p=1$. A table is presented which allows one to compare the exact and approximate $\sigma$'s for $p=1$ over a wide range of energy and scattering angles. The agreement is particularly good for large energy transfer.

## I. INTRODUCTION

THE purpose of this paper is to present a method for obtaining approximate analytic representations for classical differential scattering cross sections suitable for studying slowing down processes in radiation damage theory.[1] Briefly, this approximation will be shown to interpolate remarkably well between the impulse and hard-sphere approximations valid, respectively, for small and large angle scattering.

In Sec. II, the problem of determining an approximate relationship between the impact parameter, $b$, and the angle, $\theta$, associated with an arbitrary central repulsive force scattering of an incident atom by a target atom will be discussed.

Approximate analytic expressions for the impact parameter and differential scattering cross section will be derived in Sec. III for three types of screened Coulomb potential energy functions suggested by Brinkman and Meechan.[2] Exact solutions for the impact parameter and differential scattering cross section have been worked out for a special case of the aforementioned potential energy and a comparison between these results and those derived from the analytic approximations will be given in Sec. IV.

## II. DERIVATION OF APPROXIMATE SCATTERING EQUATIONS

Figure 1 shows the path described by an incident atom being scattered by a repulsive central force through an angle, $\theta$, by a fixed target atom. In this figure, the impact parameter is denoted by $b$ and the coordinates $(r,\phi)$ define the path of the incident atom relative to the target atom as the origin. The differential equation for the $(r,\phi)$ trajectory is given by the well-known expression[3]

$$(u')^2+u^2=b^{-2}(1-E^{-1}V), \tag{1}$$

where $u=1/r$, $V$ is the potential energy of interaction, and $E$ is the energy of the incident atom measured in the center-of-mass system. The prime on $u$ denotes differentiation with respect to $\phi$. The exact relationship between $\theta$ and $b$ is easily derived from Eq. (1) and is well known to be[3]

$$\theta=\pi-2\int_0^{u_0}du[b^{-2}(1-E^{-1}V)-u^2]^{-\frac{1}{2}}, \tag{2}$$

where $u_0$ is the zero of the integrand and physically

* This work was supported by the U. S. Atomic Energy Commission.
† Present address is Physics Department, University of California, Los Angeles, California.
[1] For a recent review article concerning the status of slowing down processes in radiation damage theory, see G. J. Dienes and G. H. Vineyard, *Radiation Effects in Solids* (Interscience Publishers, New York, 1957).
[2] J. A. Brinkman and C. J. Meechan (to be published).
[3] H. Goldstein, *Classical Mechanics* (Addison-Wesley Publishing Company, Inc., Reading, Massachusetts, 1950).